

Bidirectional Antagonistic Variable Stiffness Actuation: Analysis, Design & Implementation

Florian Petit, Maxime Chalon, Werner Friedl, Markus Grebenstein, Alin Albu-Schäffer and Gerd Hirzinger

Institute of Robotics and Mechatronics, German Aerospace Center (DLR), Wessling, Germany

E-mails: {Florian.Petit, Maxime.Chalon, Werner.Friedl, Markus.Grebenstein, Alin.Albu-Schaeffer}@dlr.de

Abstract—The variable stiffness actuation concept is considered to provide a human-friendly robot technology. This paper examines a joint concept called the bidirectional antagonistic joint which is an extension of antagonistic joints. A new operating mode called the helping mode is introduced, which increases the joint load range. Although the joint can not be pretensioned in the helping mode, it is shown that a stiffness variation is possible, assuming a suitable torque-stiffness characteristic of the elastic elements. A methodology to design such characteristics is presented along with several example cases interpreted in a torque-stiffness plot. Furthermore, a stiffness adaptation control scheme which ensures mechanism safety is described. Finally, the design methodology and the control are evaluated on an implementation of a bidirectional antagonistic joint.

I. INTRODUCTION

Classical industrial robots consist of heavy and stiff structures. They also lack the ability to perceive and react appropriately to human interaction. It is therefore inappropriate for such robots to operate in environments shared with humans. Additionally, these robots are outperformed by the human in unstructured and partially unknown environments. Several research efforts have been geared toward robots with improved performance and human-friendliness. One example is the torque-controlled lightweight robot (LWR) developed at the German Aerospace Center (DLR) [1]. The desired soft robotic features are achieved through torque control. Sensors are deployed to measure torques acting on the robot and a control loop is implemented to attain active compliant behavior. However, these systems remain mechanically stiff compared to a human arm. The software compliance is limited by sensor bandwidth and precision, model inaccuracy, and motor dynamics. While robot-human interaction has shown great promise, the high stiffness remains a challenge to be addressed when the robot mechanics itself have to be protected [2] [3]. Fast and forceful external overloads, such as rigid impacts, can exceed the load rating of the drive train, and may lead to system failure.

A technology which incorporates compliant behavior, mainly in hardware, may be utilized to overcome the drawback of the high joint stiffness. One possible solution to the problem is the variable stiffness actuation (VSA) concept, which is a topic of ongoing research [4]. In VSA, elastic elements are integrated into the joints. Due to the non-linear force-deflection characteristic of the elastic elements, the stiffness can be varied and adapted to the task at hand [5] [6] [7] [8] [9] [10]. By decoupling the internal drive train from

the external link with a passively compliant element, the joint can be protected from damage. Furthermore, it can address some safety issues for the physical human-robot interaction. The elastic elements can also be used as energy storage mechanisms to increase efficiency or link speed during task operation [11] [12] [13] [14].

Multiple variable stiffness actuators have been developed with different mechanical designs which allow the adjustment of stiffness and position of joints. One approach is to use two motors of different sizes, with one adjusting the stiffness preset and the other the position [14]. Another approach is the antagonistic setup inspired by the human muscle system. In this approach, position and stiffness adjustments are performed by a superimposed motion of both actuators. This concept has been implemented and demonstrated in [15] and [16]. However, by using electric motors in the normal antagonistic setup, only the torque of one motor is available at the link joint to compensate for an external load. The other motor torque can not be used. In order to address this drawback, the bidirectional antagonistic approach was introduced in [17] and [18]. This concept enhances the previous antagonistic setup with a bidirectional connection of each motor to the link, which enables an additional mode, called the helping mode. In the helping mode, the motors support each other to generate a higher torque at the link joint. The main advantage of the helping mode is the increased torque capability of the joint.

To our knowledge, the properties of the bidirectional antagonism, particularly regarding the helping mode, have not yet been fully exploited. Therefore this work aims to introduce its basic design, control, and stiffness properties. First, the two modes of operation, the normal- and the helping operating mode, are analyzed in detail. It is shown how to make use of them in position and stiffness control with a focus on the helping mode. One of the main findings is that the stiffness can be varied, even in the helping mode with a suitable stiffness characteristic of the joint. The design of the stiffness characteristic has been composed into a synthesis method. The results for the stiffness variation capabilities in the two modes are interpreted with the aid of a characteristic stiffness-torque plot. Furthermore, a control algorithm to ensure a safe stiffness and torque range of the mechanism is presented. Finally, the described approaches are evaluated on a prototypical implementation of a bidirectional antagonistic joint.

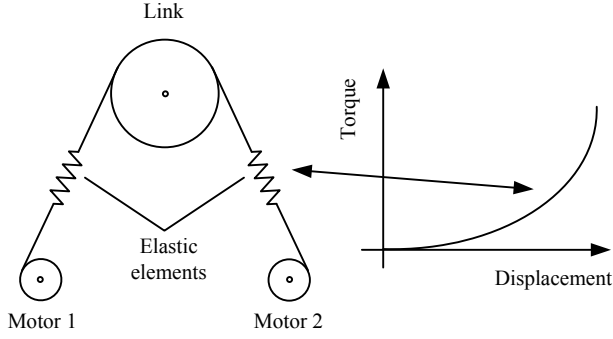


Fig. 1. On the left a normal antagonistic setup with actuators acting only in the pulling direction is shown. An increasing and convex torque-displacement profile is desired (right side), which enables the stiffness variation.

II. DESIGN

A. Variable Stiffness Actuation

Variable stiffness actuation aims to adjust the link position and its passive stiffness. In the antagonistic setup Fig. 1 (left), a non-linear torque-displacement characteristic of the elastic elements is essential for stiffness variation. This is due to the dependency of a mechanism's stiffness on the torque curve and the applied torque. The stiffness is defined as

$$k(\theta) := \frac{\partial \tau(\theta)}{\partial \theta}. \quad (1)$$

For this work a torque-displacement curve is used for the elastic elements, with an exclusively increasing ($\partial f / \partial x > 0$) and convex profile ($\partial^2 f / \partial x^2 > 0$), see Fig. 1 (right). To change the joint stiffness, the elastic elements are elongated by driving the motors in opposite directions in the antagonistic setup. This increases the applied force to the elastic member. As a result the stiffness of the link is increased, too.

B. The bidirectional antagonism

Unlike the human muscle, electric motors are able to act in two directions. This bidirectionality allows the extension from the normal antagonism into a bidirectional antagonism: Each motor is connected bidirectionally to the link to drive it in both directions, and the two actuator torques add up to generate the overall link torque. In the proposed setup, the bidirectional antagonism can be achieved by replacing the single string between one motor and the link by a complete loop around them. Please note that the cables are rigidly connected to the link and the motor. Still, elastic elements partially decouple the motors from the link, see Fig. 2 (left). One motor with its two elastic elements is called a 'motor-spring unit' or a 'side' of the bidirectional antagonistic setup.

First, the torque composition of one side is discussed in more detail. This is followed by an explanation of the torque and stiffness properties of both sides.

Motor-spring unit torque composition The elastic elements in between the link and the motors change their lengths (non-linear!) with respect to the applied force. Conversely, the applied torque can be estimated via the spring

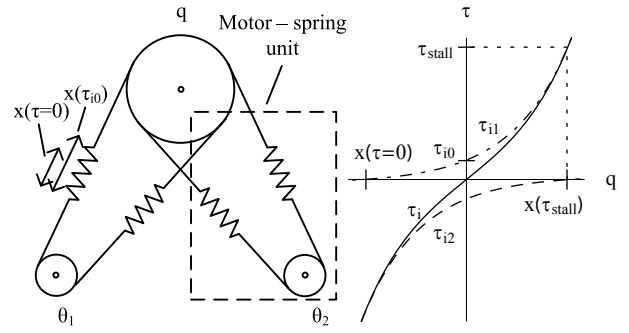


Fig. 2. The bidirectional antagonistic setup can be seen on the left side. A complete loop connects the motors and the joint, which results in the desired z-shaped torque-displacement curve. This allows the motors to generate torques in both directions at the joint. How the overall torque curve adds up is shown on the right. The single non-linear elastic elements are pretensioned by an internal torque τ_{i0} .

deflection as presented in [19] for linear springs. This mechanism, in conjunction with position controlled motors, enables the use of the motor-spring unit as torque source.

The torque generated by one motor-spring unit

$$\tau_i = \tau_{i1}(\theta_i, q) + \tau_{i2}(\theta_i, q) \quad (2)$$

consists of the parallel connection between the two single springs with torques $\tau_{i1}(\theta_i, q)$ and $\tau_{i2}(\theta_i, q)$ depending on the motor position θ_i and the joint position q . This results in a z-shaped torque curve, see Fig. 2 (right). In the following, only the torques τ_i of one motor-spring unit will be referenced.

To avoid slack in the mechanism, the springs in one loop are constantly pretensioned. The internal pretension $\tau_{i0} = \tau(x_{i0})$ (x_{i0} is the related displacement) of the single springs must be sufficient such that they do not relax even under the motor stall torque τ_{stall} , therefore $x_{i0} = \frac{x(\tau_{\text{stall}})}{2}$. $x(\tau)$ is the displacement of the spring due to the applied torque τ . This ensures that the springs are able to transmit the bidirectional torque of each motor to the joint, for any achievable operating point.

Joint torque & stiffness composition Both actuators in the bidirectional setup are able to contribute to the overall joint torque τ :

$$\tau = \tau_1 + \tau_2 \quad |\tau_i| \leq \tau_{\text{stall}} \quad \forall i \quad (3)$$

where τ_1 and τ_2 are the torques generated by each motor-spring unit. In contrast to that, the normal antagonism has the limitations $\tau_{\text{stall}} \leq \tau_1 \leq 0$ and $0 \leq \tau_2 \leq \tau_{\text{stall}}$.

The overall link stiffness k is summed up to

$$k = k_1(\tau_1) + k_2(\tau_2) \quad 0 \leq k_i(\tau_i) \quad \forall \tau_i \quad (4)$$

where $k_1(\tau_1)$ and $k_2(\tau_2)$ are the stiffness of the two motor-spring units.

III. OPERATING MODES

The modification towards the bidirectional antagonism allows to use the operating mode of the standard antagonistic setup (called 'normal mode') and enables an additional

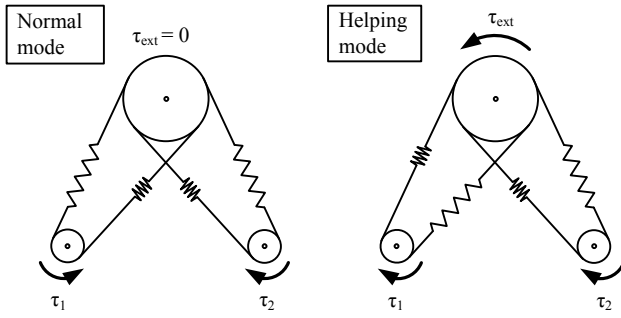


Fig. 3. The modes of operation of the bidirectional antagonistic setup. Each motor is able to apply bidirectional torques at the links. In the normal mode, the units generate torques which cancel each other, whereas the link stiffness is increased. In the helping mode, the motors support each other and generate a higher external torque.

'helping mode'. In the helping mode the motors are able to support each other, see Fig. 3. While the normal mode has a broad stiffness adjustment capability for low external torques, the helping mode significantly extends the torque operating region still allowing some stiffness variation.

A. Normal antagonistic mode

In this mode, the torques generated have different signs. Its magnitude can be equal or different:

- When the torques are of equal magnitude but have opposing signs, e.g. $\tau_1 = -\tau_2 = \tau_0$ (τ_0 is the torque used for pretension), no net link torque is generated as they compensate for each other. This produces a zero link torque in accordance with (3).

$$\tau = \tau_1 + \tau_2 = 0$$

Although no external torque is generated, the link stiffness k is increased, This is due to the fact that stiffness of the elastic elements is depending upon the torques applied.

$$k = k_1(\tau_1) + k_2(\tau_2) > k_1(0) + k_2(0)$$

$k_i(0)$ is the stiffness of the units for the unloaded case. Therefore, internal opposing torques can be used to control the stiffness of the joint in absence of an external torque. Control algorithms to adjust the stiffness independent of the position have been presented in [17], [18] and [20]. In the following, this operation to increase stiffness by internal torques is referred to as 'pretensioning' of the joint.

- Torques of different magnitude and opposing signs, e.g. $\tau_1 < 0 < \tau_2$, compensate for each other up to a certain limit. However, the difference of the two torques generates an external torque at the link. For example

$$\underbrace{\tau_0 + \tau_{\text{ext}}}_{\tau_1} - \underbrace{\tau_0}_{\tau_2} = \tau_{\text{ext}} = \tau$$

with τ_{ext} as the torque available at the link. This case is the solution of (3) for a link torque and internal torques of different magnitude but still different signs.

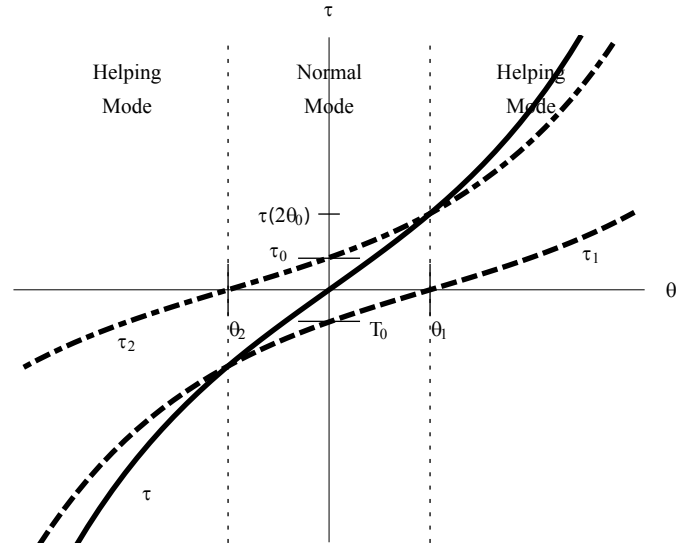


Fig. 4. A plot of the two spring-motor unit torques (dashed) and the resulting link torque (thick). The unit torque curves have moved out of the center and summed up to a steeper link torque curve. Once the actual torque operating point exceeds the point θ_i , the passive transition from the normal to the helping mode is performed.

Figure 4 shows the result of pretensioning of the two motor-spring units for the overall torque. The two single torque curves τ_i are normally both centered at $\theta = 0$ in the relaxed case. By pretensioning the units by moving the motors to $\theta_1 = -\theta_2 = \theta_0$, internal torques τ_0 are generated. The internal torques compensate for each other, but increase the stiffness. Therefore the torque curves τ_i are shifted symmetrically from the center, which results in a steeper link torque curve τ .

If no external torque is applied to the joint, the operating point remains at the origin of the torque-displacement curve on the link torque curve. By increasing the external torque, the operating point slides along the torque curve τ . Once the pretension torque $\tau = \tau_i(2\theta_0)$ boundary is exceeded, the motor torques no longer working against each other. This means that the mechanism is no longer in the normal mode, as this mode is defined to have opposing motor torques. At this point the helping mode begins. This is another possible outcome of (3) which is discussed in the next Section.

B. Helping antagonistic mode

The helping mode uses torques in the same direction to allow the motors to support each other. Therefore the motor-spring unit torques are $\tau_i < 0$ or $0 < \tau_i$. To fulfill (3), an external torque is essentially required and has to be directed against the τ_i 's, therefore

$$\tau = \tau_{\text{ext}} = \sum_i \tau_i \quad (5)$$

see Fig. 3 (right). Without any external torque the helping mode does not activate.

The helping mode allows the creation of a torque at the link, which can be up to twice the stall torque of a

single motor, as long as no internal torque is generated for pretensioning.

$$\tau \leq 2 \tau_{\text{stall}}$$

This cooperation of the two motors allows not only for a larger torque range of the setup, but also makes a stiffness variation possible: An external load can be compensated by motor-spring unit torques of different magnitude. By varying the ratio of the magnitudes also different unit stiffness is generated, which results in a different link stiffness. To exploit the stiffness variation capabilities during the helping mode, the following load distribution approach is used.

Load distribution in the helping mode The load is distributed between the two motors:

$$\begin{aligned} \tau &= \alpha \tau_{\text{ext}} + (1 - \alpha) \tau_{\text{ext}} \\ \alpha &\in [0, 1] \end{aligned} \quad (6)$$

The coefficient α indicates the load distribution. τ_{ext} is the external load. With (3) the motor torques become

$$\tau_1 = \alpha \tau_{\text{ext}}, \quad (7)$$

and

$$\tau_2 = (1 - \alpha) \tau_{\text{ext}}. \quad (8)$$

The according stiffness is

$$k = k_1(\alpha \tau_{\text{ext}}) + k_2((1 - \alpha) \tau_{\text{ext}}).$$

Two extreme cases of the load sharing can be imagined: First, when only one motor compensates for the complete external load, while the second motor is idle ($\alpha = 1$ or $\alpha = 0$). Second, when the two motors contribute the equal amount to the join torque ($\alpha = \frac{1}{2}$). These two cases describe the limits for the stiffness variation: The lowest stiffness is achieved for the lowest motor-spring unit torques, therefore equal sharing. The highest stiffness is achieved by generating the highest possible torque, therefore operating one unit at its load limit¹. However, the stiffness variation capability depends on the exact torque-stiffness curve. Further evaluation and a synthesis method are presented in Section IV.

IV. STIFFNESS CHARACTERISTICS

As the static case is investigated, the link position can always be controlled, independent of the system state. This is not the case for the achievable stiffness as it depends on the applied external torque and the current operating mode. This has two major consequences. First, stiffness control has to be extended to take account for the actual external load. Such a controller is introduced in Section V. Second, the use of the limitation on the zero link torque case to characterize the stiffness ability of a variable stiffness joint is too much of an abstraction, and does not adequately represent its abilities. A stiffness-torque plot provides a better description of a joint's specification. The properties of such a plot are discussed here.

¹This is due to the monotonic increase of the torque-stiffness characteristics

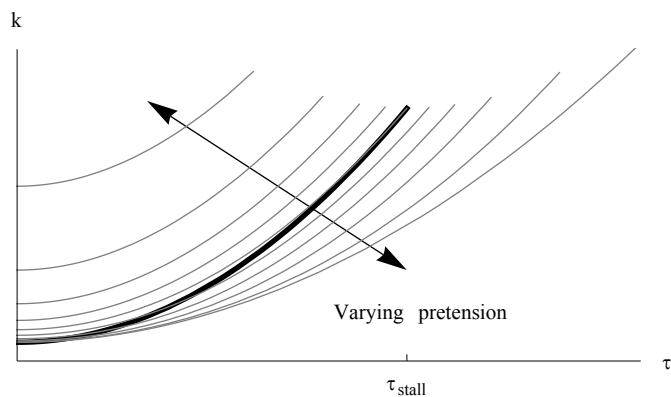


Fig. 5. A plot of a stiffness-torque curve. The thin lines are the stiffness curves for increasing pretensioning of the motors. The thick line represents the boundary between the normal and the helping mode. The maximum achievable link torque is limited by the stall torque of a spring-motor unit. The helping mode allows the link torque to be twice the motor torque.

A. Characteristics interpretation

In Fig. 5 an arbitrary stiffness-torque curve for the bidirectional antagonistic setup is shown. It can be interpreted as follows:

Positive link torques are plotted along the horizontal axis. The plot is symmetric at the vertical axis, which shows increasing stiffness for zero external torque. In contrast to Fig. 4, where only the resulting torque curve for one pretension torque is shown, this plot contains all available stiffness-torque curves. The family of curves arises from different pretensions of the mechanism. The lowest curve is equal to no pretension (highest achievable link torque) and the highest curve equals the highest possible pretension (lowest achievable link torque). The stiffness curves are cut off when the stall torque of one motor is exceeded.

The bold printed curve in the plot is the boundary between the normal and the helping mode. Upon crossing it, the motor-spring units no longer work against each other, but rather support each other, as illustrated in Section III-B, Fig. 4. However, some of the stiffness curves cross this boundary. This transition from normal- to helping mode happens passively when the external load increases. During operation, the crossing of the boundary will happen smoothly.

As an operating point approaches the end of a curve, the mechanism operates increasingly close to one unit stall torque. To further load the joint, it has to be switched to a curve with lower stiffness. In the normal mode, this switching means the reduction of the pretension of the motors to make available more torque at the link. In the helping mode, this switching means a more equal distribution of the link load between the two motors. When the link load is distributed equally between the two motors ($\alpha = \frac{1}{2}$), the highest torque is available at the link. A stiffness adaptation control scheme to switch between the stiffness curves is presented in Section V.

B. Designing the stiffness characteristics

It is shown in Section III, that a stiffness change is even possible during the helping mode. In this Section, several non-linear joint stiffness characteristics are synthesized and analyzed for their stiffness variation capabilities.

For the helping antagonistic mode, a stiffness change can be managed by altering the two motor torques, as described by (6). The two extreme cases ($\alpha = \frac{1}{2}$ and $\alpha = 1|0$) result in the lower and upper boundaries for achievable stiffness. With these boundaries, the possible stiffness variation range of the joint in the normal and helping mode can be derived. The synthesis uses a desired stiffness-torque curve as a starting point. Afterwards, the necessary torque-displacement curve is deduced, as required for a mechanical implementation.

The synthesis starts by defining a desired stiffness-torque curve

$$k = D(\tau)$$

where $D(\tau)$ is the selected design function. Given (1), it is possible to formulate the following differential equation:

$$\frac{\partial \tau(\theta)}{\partial \theta} = D(\tau(\theta))$$

By solving this equation, a solution for the torque and stiffness curve can be obtained. In order to obtain an analytical solution, $D(\tau)$ may not be of arbitrary shape. However, there exist solutions for several prototype cases as discussed below.

1) *Linear torque-stiffness relation:* $k(\tau) = c\tau$: The first desired characteristic is a linear increasing stiffness-torque curve

$$k(\tau) = c\tau \quad (9)$$

where c is a positive real constant of unit $[1/rad]$. It follows

$$k(\tau) = \frac{\partial \tau(\theta)}{\partial \theta} = c\tau(\theta)$$

The result for the torque-displacement curve is

$$\tau(\theta) = \frac{d}{c} e^{c\theta}$$

with d $[Nm/rad]$ also a positive real constant and the corresponding stiffness curve is

$$k(\theta) = \frac{\partial \tau(\theta)}{\partial \theta} = d e^{c\theta}$$

In this case, stiffness changes linearly with torque. As a result, varying the load between the two motors has no effect, see Fig. 6 (left). This is due to the fact that any linear combination of the single stiffness always adds up to the same link stiffness, as can be easily verified using (4), (7), (8) and (9):

$$k = c\tau_1 + c\tau_2 = c\alpha\tau_{\text{ext}} + c(1-\alpha)\tau_{\text{ext}} = c\tau_{\text{ext}}$$

Thus, the linear stiffness-torque characteristic is not a good choice if a stiffness variation is desired in the helping mode. To guarantee a large stiffness variation capability in the helping mode, the stiffness change of each actuator should be high for changing torques. Therefore, $D(\tau)$ should be as non-linear as possible. This will be evaluated in the next Subsections.

Please note that $\tau(\theta) = e^{c\theta}$ is not z-shaped as required in Section II-B. The real implemented torque curve is $\tau = a(e^{b\theta} - e^{-b\theta})$, with a and $b \in \mathfrak{R}^+$, what results in a z-shaped torque curve. Nonetheless, the assumption of the ideal torque curve holds for a wide range of θ values.

2) *Quadratic torque-stiffness relation* $k(\tau) = cd(1 + \frac{\tau^2}{c^2})$: A moderate non-linear characteristic is a quadratically increasing stiffness curve:

$$k(\tau) = cd(1 + \frac{\tau^2}{c^2}), \quad (10)$$

c $[Nm]$ and d $[1/rad]$ real positive constants. Furthermore

$$\tau(\theta) = c \tan(d\theta).$$

For the stiffness-displacement curve the following relation holds

$$k(\theta) = \frac{\partial \tau(\theta)}{\partial \theta} = cd \frac{1}{\cos^2(d\theta)}.$$

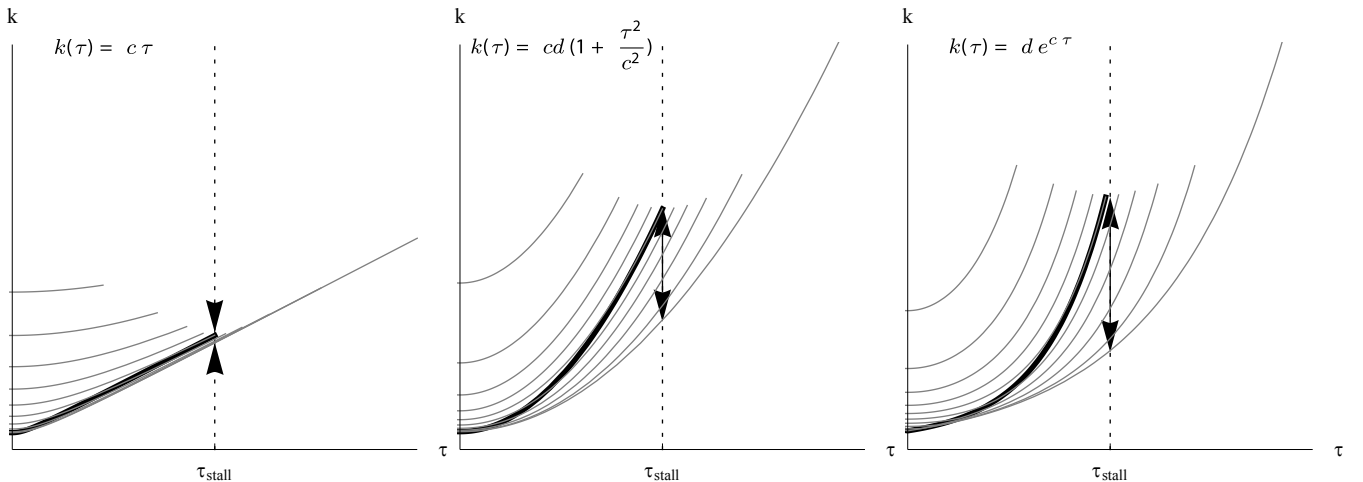


Fig. 6. The three torque-stiffness curves (see Sections IV-B.1, IV-B.2, IV-B.3). The thick line is the boundary between the normal and the helping mode region. The arrows show the available stiffness range of the helping mode region at $\tau = \tau_{\text{stall}}$. The increasing stiffness range from the linear to the exponential plot can be clearly seen.

This quadratic stiffness curve already demonstrates a reasonable achievable stiffness range for the helping antagonistic case, see Fig. 6 (middle).

3) *Exponential torque-stiffness relation:* $k(\tau) = d e^c \tau$: An even more pronounced non-linearity consists of an exponential relationship. The desired stiffness-torque curve is chosen to be

$$k(\tau) = d e^c \tau. \quad (11)$$

$c[1/Nm]$ and $d[Nm/rad]$ are real positive constants, again. The torque-displacement curve is

$$\tau(\theta) = -\frac{1}{c} \ln(-cd \theta) \quad \theta < 0,$$

with the stiffness-displacement relationship

$$k(\theta) = \frac{\partial \tau(\theta)}{\partial \theta} = -\frac{1}{c \theta}$$

As the torque curve $\tau(\theta)$ is only defined for negative displacements, this result has to be modified for a practical realization:

$$\tau = -\text{sgn}(\theta) a \ln(-\text{sgn}(\theta) \theta + b) + \text{sgn}(\theta) a \ln(b)$$

With a and $b \in \mathfrak{R}^+$. This is a shift of the torque-displacement curve along the horizontal axis and does not change the desired property of (11). The result can be seen in Fig. 6 (right).

V. STIFFNESS ADAPTATION SCHEME

The bidirectional antagonism allows the link torque to be up to twice the maximum motor torque. Through pretensioning in the normal mode, or unequal loading in the helping mode ($\alpha \neq \frac{1}{2}$), part of the motor torque is used to increase the link stiffness (τ_0). As a consequence, the available joint torque component $\tau_{i,\text{ext}}$ of τ_i is reduced, as the follow must hold:

$$\tau_i = \tau_0 + \tau_{i,\text{ext}} < \tau_{\text{stall}}$$

During a task it is important to make the full joint torque $\tau = 2\tau_{\text{stall}}$ available, even if it requires the reduction of the joint stiffness by lowering the pretension τ_0 . The pretension can be reduced by switching to a lower stiffness curve as it is described in Section IV. Once the pretension is at its minimum value $\tau_0 = 0$, both motors support each other and the maximal joint torque is available.

The adaptation scheme presented here follows the described concept to reduce the motor load caused by pretension: The current motor-spring unit torque τ_i is estimated by the force sensing capabilities of the elastic elements. If this torque exceeds a defined upper boundary torque τ_{lim} , the commanded pretension θ_c (motor position!) is reduced below the desired value θ_0 until a safe operating region is reached.

$$\theta_c = \max(0, \theta_0 - \sum_i \theta(K_i \max(0, \tau_i - \tau_{\text{lim}})))$$

K_i is calculated to keep the unit torques below the motor stall torque τ_{stall}

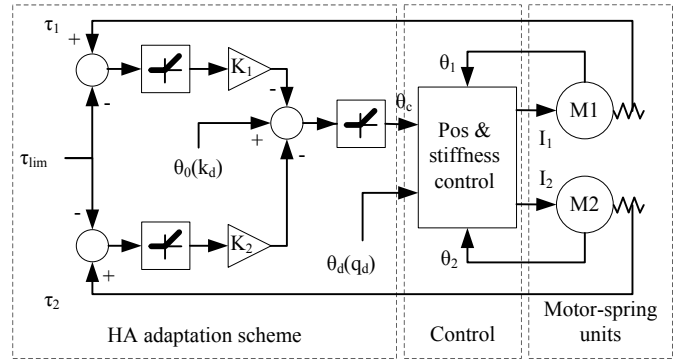


Fig. 7. The helping antagonism stiffness adaptation scheme.

Figure 7 shows a signal flow graph of the helping antagonism stiffness adaptation scheme for both motor-spring units. The stiffness is kept as close as possible to the commanded value within a safety margin to ensure the protection of the motor-spring units. The motors may be overloaded independently, therefore both motor-spring unit torques have to be considered for the adaptation of the pretension. Please note, that although only one motor-spring unit will be overloaded at once, the stiffness has to be reduced by a symmetric motion of the motors to ensure the desired link position.

VI. EXPERIMENTS

Currently DLR is developing a robotic hand-arm system with VSA [21]. In this context, a bidirectional helping antagonism testbed was developed at the institute [17]. The setup design is similar to the abstractions shown in Fig. 2 and can be seen in Fig. 8. Cables are used to connect

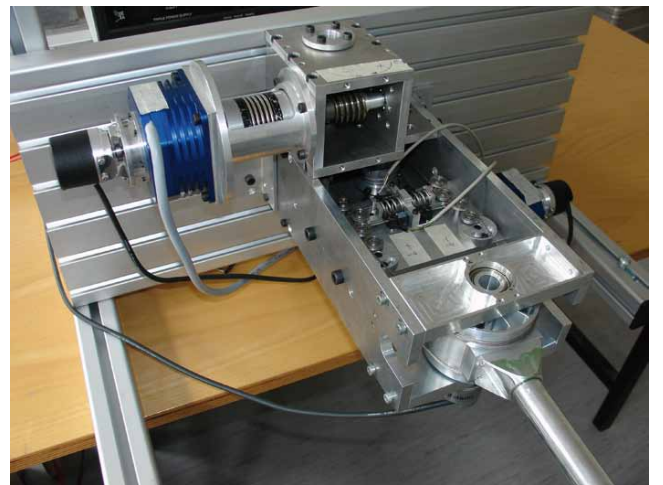


Fig. 8. The bidirectional antagonistic joint prototype. Only one motor-spring unit is visible completely, as the other one points downwards. To the far left the DLR ILM motors with attached encoders are visible. The worm gear in the square box connects the motor to the tendon mechanism. In the lower right corner the link rod can be seen. The non-linear elastic element is located between the worm gear and the link.

the drives to the springs and the link. Two DLR ILM 70iH electric motors in combination with two Sensodrive Unireg 12 motor controllers are position controlled. The motors are equipped with encoders with 3600 increments per revolution. Additionally, a non-backdrivable worm gear yields a 30/1 transmission.

A. Non-linear elastic element implementation & calibration

The variable stiffness elements are implemented by a variable cable guiding, see Fig. 9. The non-linear spring mechanism consists of two fixed and one movable pulley. By increasing the string tension, the movable pulley deflects the linear spring. Due to the geometrical change, a non-linear relation of the string force - string displacement is obtained.

To estimate the applied force by the elastic elements (see II-B) the spring deflection is measured by an analog linear potentiometer. The force-displacement characteristic is calibrated initially by a reference measurement: Forces are applied and measured by an external strain gauge and the resulting displacement of each spring element is recorded. To later infer a measured spring displacement to the applied force, the obtained data is fitted to a fourth order polynomial. In the composed setup, the displacement of the four elastic elements allow to estimate the applied external torque, compare (2) and (3).

B. Setup torque-stiffness characteristic

To achieve an outline of the torque-stiffness characteristic of the setup, several torque-displacement curves with varying pretensions were recorded. The applied link torque is estimated by the elastic element deflection. The joint stiffness is calculated based on (1) and the torque estimation fit. The resulting torque-stiffness plot can be seen in Fig. 10.

C. Stiffness adaptation scheme

The performance of the stiffness adaptation control scheme was tested experimentally. Figure 11 shows the result in a torque-stiffness plot and Fig. 12 shows the corresponding motor position over time. A task was simulated with the following sequence:

- A The joint is in its unloaded initial position.
- B A desired pretension value k_d is specified what results in a motor position change to θ_0 thus a increased stiffness. The joint is loaded what lets the system state slide along a stiffness curve until

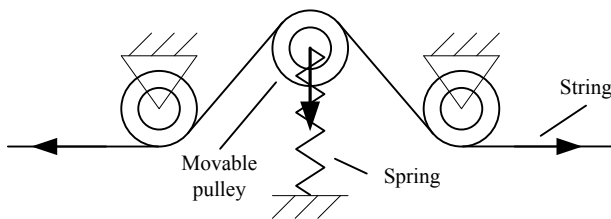


Fig. 9. The non-linear spring realization: a pulley deflects a linear spring relative to the string length given by the motor and link geometry. The relationship between string length and pulley deflection is non-linear.

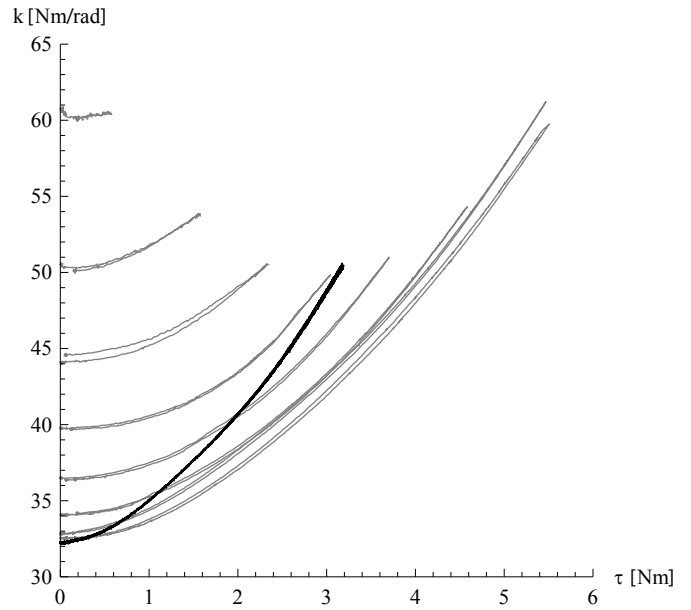


Fig. 10. The torque-displacement plot for the experimental test joint. The torques were estimated by the elastic element displacement. Increasing pretension results in curves with higher stiffness at zero torque. The thick black line is the boundary between the normal and the helping mode.

- C is reached. Here, one unit is loaded with the limit motor torque τ_{lim} . When the joint is further loaded, the stiffness adaptation scheme will reduce the pretension to keep the unit torques in the allowed region. At
- D the pretension is reduced to $\theta_c = 0$. Thus, twice the motor stall torque is available at the link.

Please note, that the transition from normal- to the helping mode happens smoothly, as expected.

VII. CONCLUSION

The principle of the bidirectional antagonistic joint and especially the helping operating mode together with design methodologies were presented in this paper. The helping mode has substantial advantages in increasing the joint load and the stiffness range compared to the normal operating mode in the pure antagonistic setup. The importance of the chosen stiffness curve for the stiffness variation capability in the helping mode is shown. The synthesis method presented allows to analyze various torque-stiffness characteristics. The curves differ in the resulting absolute stiffness range and the adjustable resolution (compare also [22]).

Furthermore, a stiffness adaptation control scheme was presented to ensure a safe operating region of the bidirectional antagonistic joint.

The experimental part presents the developed bidirectional antagonistic joint. The in afore shown theoretical findings, like the torque-stiffness characteristic of the joint or the passive transition from normal- to the helping mode, are evaluated on the joint. Finally, a experimentally simulated task shows the functionality of the presented helping antagonism control scheme.

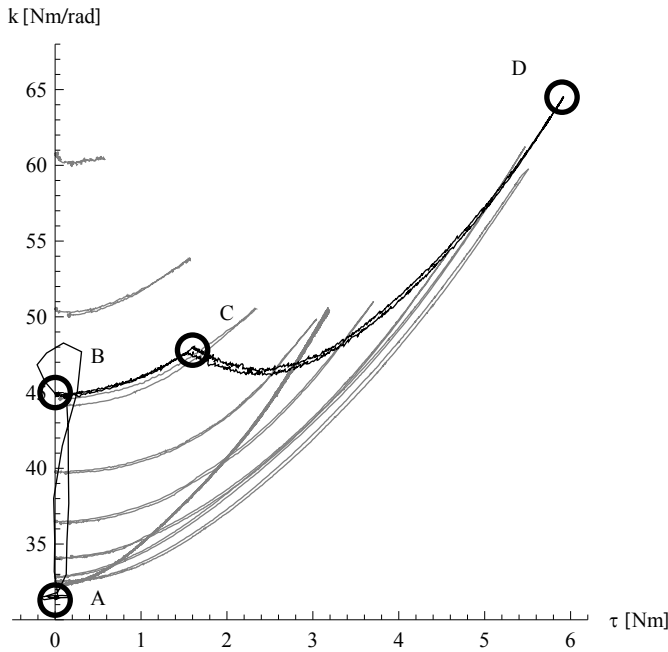


Fig. 11. The adaptation algorithm during task execution interpreted in a torque-stiffness plot. The unloaded mechanism A gets pretensioned to B. Loading the joint moves the operating point to C. When the joint external torque is increased further, the stiffness is reduced by the HA adaptation scheme to keep the mechanism in a safe region of operation. No pretension and the maximal link torque is achieved at D.

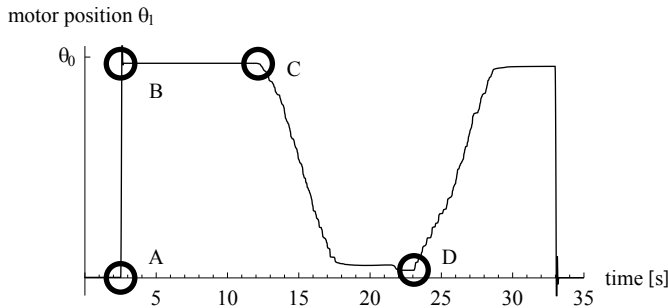


Fig. 12. The adaptation algorithm during task execution interpreted in a motor position plot, compare Fig. 11. The motors generate the desired pretension by positioning at θ_0 . Once the unit torque is exceeding the allowed value at C, the pretension position gets reduced to the minimal value D.

Please note, besides of the necessity of a non-linear stiffness-torque characteristic for stiffness adjustment in the helping mode, the desired stiffness characteristic seems to be task dependent. A global advantageous characteristics can not be given at this point. However, this is a very interesting topic and will be addressed in further research.

VIII. ACKNOWLEDGMENTS

This work has been partially funded by the European Commissions Sixth Framework Programme as part of the project PHRIENDS under grant no. 045359 and the project VIATORS under grant no. 231554.

REFERENCES

- [1] A. Albu-Schäfer, O. Eiberger, M. Grebenstein, S. Haddadin, C. Ott, T. Wimböck, S. Wolf, and G. Hirzinger, "From torque feedback-controlled lightweight robots to intrinsically compliant systems," *IEEE Robotics and Automation Magazine*, vol. 15, no. 3, pp. 20–30, 2008.
- [2] S. Haddadin, T. Laue, U. Frese, S. Wolf, A. Albu-Schäfer, and G. Hirzinger, "Kick it like a safe robot: Requirements for 2050," *Robotics and Autonomous Systems*, vol. 57, pp. 761–775, 2009.
- [3] S. Haddadin, A. Albu-Schäfer, and G. Hirzinger, "Requirements for safe robots: Measurements, analysis & new insights," *accepted for publication: Int. J. of Robotics Research*, 2009.
- [4] "Physical Human-Robot Interaction: DepENDability and Safety," <http://www.phriends.eu>.
- [5] K. Laurin-Kovitz, J. Colgate, and S. Carnes, "Design of components for programmable passive impedance," in *Proc. of the IEEE International Conference on Robotics and Automation*, Apr 1991, pp. 1476–1481 vol.2.
- [6] T. Morita and S. Sugano, "Design and development of a new robot joint using a mechanical impedance adjuster," in *Proc. of the IEEE International Conference on Robotics and Automation*, vol. 3, May 1995, pp. 2469–2475 vol.3.
- [7] M. Okada, Y. Nakamura, and S. Ban, "Design of programmable passive compliance shoulder mechanism," in *Proc. of the IEEE International Conference on Robotics and Automation*, vol. 1, 2001, pp. 348–353 vol.1.
- [8] K. Koganezawa, "Mechanical stiffness control for antagonistically driven joints," in *Proc. of the IEEE/RSJ International Conference on Intelligent Robots and Systems*, Aug. 2005, pp. 1544–1551.
- [9] G. Tonietti, R. Schiavi, and A. Bicchi, "Design and control of a variable stiffness actuator for safe and fast physical human/robot interaction," in *Proc. of the IEEE International Conference on Robotics and Automation*, 2005, pp. 528–533.
- [10] O. Eiberger, S. Haddadin, M. Weis, A. Albu-Schäfer, and G. Hirzinger, "On joint design with intrinsic variable compliance: Derivation of the DLR QA-joint," *IEEE Int. Conf. on Robotics and Automation (ICRA2010)*, Anchorage, Alaska, 2010.
- [11] M. Raibert, *Legged Robots that Balance*. MIT Press, 1986.
- [12] J. W. Hurst, J. Chestnutt, and A. Rizzi, "An actuator with physically variable stiffness for highly dynamic legged locomotion," in *Proc. of the IEEE International Conference on Robotics and Automation*, vol. 5, May 2004, pp. 4662 – 4667.
- [13] B. Vanderborght, B. Verrelst, R. Van Ham, M. Van Damme, D. Lefeber, B. M. Y. Duran, and P. Beyl, "Exploiting natural dynamics to reduce energy consumption by controlling the compliance of soft actuators," *Int. J. Rob. Res.*, vol. 25, no. 4, pp. 343–358, 2006.
- [14] S. Wolf and G. Hirzinger, "A new variable stiffness design: Matching requirements of the next robot generation," in *Proc. of the IEEE International Conference on Robotics and Automation*, Pasadena, CA, USA, 2008, pp. 1741–1746.
- [15] K. Koganezawa, Y. Watanabe, and N. Shimizu, "Antagonistic muscle-like actuator and its application to multi-dof forearm prosthesis," *Advanced Robotics*, vol. 12, no. 7, pp. 771–789, 1999.
- [16] S. A. Migliore, E. A. Brown, and S. P. DeWeerth, "Biologically inspired joint stiffness control," in *Proc. of the IEEE/RSJ International Conference on Intelligent Robots and Systems*, 2005, pp. 4519–4524.
- [17] M. Grebenstein, "Antagonistische Schwenkvorrichtung," German Patent No. DE 10 2006 016 958 A1, 2006.
- [18] R. Schiavi, G. Grioli, S. Sen, and A. Bicchi, "VSA-II: a novel prototype of variable stiffness actuator for safe and performing robots interacting with humans," in *Proc. of the IEEE International Conference on Robotics and Automation*, 2008, pp. 2171–2176.
- [19] G. A. Pratt and M. M. Williamson, "Series elastic actuators," in *Proc. of the IEEE/RSJ International Conference on Intelligent Robots and Systems*, Pittsburgh, PA, USA, 1995, pp. 399–406.
- [20] A. D. Luca, F. Flacco, A. Bicchi, and R. Schiavi, "Nonlinear decoupled motion-stiffness control and collision detection/reaction for the VSA-II variable stiffness device," in *Proc. of the IEEE/RSJ International Conference on Intelligent Robots and Systems*, 2009.
- [21] M. Grebenstein and P. van der Smagt, "Antagonism for a highly anthropomorphic hand/arm system," *Advanced Robotics*, no. 22, pp. 39 – 55, 2008.
- [22] M. Chalon, T. Wimböck, and G. Hirzinger, "Torque and workspace analysis for flexible tendon driven mechanisms," *IEEE Int. Conf. on Robotics and Automation (ICRA2010)*, Anchorage, Alaska, 2010.